Dynamical glass transition: critical temperature T_c and memory kernel in MD-simulated Ni$_{0.8}$Zr$_{0.2}$

A.B. Mutiara

Graduate Program in Information System, Gunadarma University,
Jl. Margonda Raya 100, Depok 16424, Indonesian.

(Dated: February 5, 2008)

We use molecular dynamics computer simulations to investigate a critical temperature T_c for a dynamical glass transition as proposed by the mode-coupling theory (MCT) of dense liquids in a glass forming Ni$_{0.8}$Zr$_{0.2}$-system. The critical temperature T_c are analyzed from different quantities and checked the consistency of the estimated values, i.e. from (i) the non-vanishing nonergodicity parameters as asymptotic solutions of the MCT equations in the arrested state, (ii) the $\mathbf{g}_m$-parameters describing the approach of the melt towards the arrested state on the ergodic side, (iii) the diffusion coefficients in the melt. The resulting T_c values are found to agree within about 10 %.

I. INTRODUCTION

The transition from a liquid to an amorphous solid that sometimes occurs upon cooling remains one of the largely unresolved problems of statistical physics [1, 2]. At the experimental level, the so-called glass transition is generally associated with a sharp increase in the characteristic relaxation times of the system, and a concomitant departure of laboratory measurements from equilibrium. At the theoretical level, it has been proposed that the transition from a liquid to a glassy state is triggered by an underlying thermodynamic (equilibrium) transition [3]; in that view, an "ideal" glass transition is believed to occur at the so-called Kauzmann temperature, T_K. At T_K, it is proposed that only one minimum-energy basin of attraction is accessible to the system. One of the first arguments of this type is due to Gibbs and diMarzio [4], but more recent studies using replica methods have yielded evidence in support of such a transition in Lennard-Jones glass formers [3, 5, 6]. These observations have been called into question by experimental data and recent results of simulations of polydisperse hard-core disks, which have failed to detect any evidence of a thermodynamic transition up to extremely high packing fractions [7]. One of the questions that arises is therefore whether the discrepancies between the reported simulated behavior of hard-disk and soft-sphere systems is due to fundamental differences in the models, or whether they are a consequence of inappropriate sampling at low temperatures and high densities.

Different, alternative theoretical considerations have attempted to establish a connection between glass transition phenomena and the rapid increase in relaxation times that arises in the vicinity of a theoretical critical temperature (the so-called "mode-coupling" temperature, T_{MCT}), thereby giving rise to a "kinetic" or "dynamic" transition [8]. In recent years, both viewpoints have received some support from molecular simulations. Many of these simulations have been conducted in the context of models introduced by Stillinger and Weber and by Kob and Andersen [9]; such models have been employed in a number of studies that have helped shape our current views about the glass transition [5, 10, 11, 12, 13, 14].

In its simplest ("idealized") version, firstly analyzed in the "schematic" approach by Bengtzelius et al. [16] and independently by Leutheusser [17], the MCT predicts a transition from a high temperature liquid ("ergodic") state to a low temperature arrested ("nonergodic") state at a critical temperature T_c. Including transversale currents as additional hydrodynamic variables, the full MCT shows no longer a sharp transition at T_c but all structural correlations decay in a final α-process [18]. Similar effects are expected from inclusion of thermally activated matter transport, that means diffusion in the arrested state [19, 20].

In the full MCT, the remainders of the transition and the value of T_c have to be evaluated, e.g., from the approach of the undercooled melt towards the idealized arrested state, either by analyzing the time and temperature dependence in the β-regime of the structural fluctuation dynamics [21, 22, 23] or by evaluating the temperature dependence of the so-called $\mathbf{g}_m$-parameter [24, 25]. There are further posibilities to estimates T_c, e.g., from the temperature dependence of the diffusion coefficients or the relaxation time of the final α-decay in the melt, as these quantities for $T > T_c$ display a critical behaviour $|T - T_c|^{\pm\gamma}$. However, only crude estimates of T_c can be obtained from these quantities, since near T_c the critical behaviour is masked by the effects of transversale currents and thermally activated matter transport, as mentioned above.

On the other hand, as emphasized and applied in [26, 27, 28], the value of T_c predicted by the idealized MCT can be calculated once the partial structure factors of the system and their temperature dependence are sufficiently well known. Besides temperature and particle concentration, the partial structure factors are the only significant quantities which enter the equations of the so-called nonergodicity parameters of the system. The latter vanish identically for temperatures above T_c and their calculation thus allows a rather precise determination of the critical temperature predicted by the idealized theory.

At this stage it is tempting to consider how well the estimates of T_c from different approaches fit together and whether the T_c estimate from the nonergodicity parameters of the idealized MCT compares to the values from the full MCT. Regarding this, we here investigate a molecular dynamics (MD) simulation model adapted to the glass-forming $Ni_{0.8}Zr_{0.2}$ transition metal system. The Ni_xZr_{1-x}-system is well studied by experiments [29, 30] and by MD-simulations [31, 32, 33, 34, 35, 36, 37, 38, 39], as it is a rather interesting system whose components are important constituents of a number of multi-component 'massive' metallic glasses. In the present contribution we consider, in particular, the $x = 0.8$ composition and concentrate on the determination of T_c from evaluating and analyzing the nonergodicity parameter, the $\mathbf{g}_m(T)$-parameter in the ergodic regime, and the diffusion coefficients.

Our paper is organized as follows: In section II, we present the model and give some details of the computations. Section III. gives a brief discussion of some aspects of the mode coupling theory as used here. Results of our MD-simulations and their analysis are then presented and discussed in Section IV.

II. SIMULATIONS

The present simulations are carried out as state-of-the-art isothermal-isobaric (N, T, p) calculations. The Newtonian equations of $N = 648$ atoms (518 Ni and 130 Zr) are numerically integrated by a fifth order predictor-corrector algorithm with time step $\Delta t = 2.5 \ 10^{-15}$s in a cubic volume with periodic boundary conditions and variable box length L. With regard to the electron theoretical description of the interatomic potentials in transition metal alloys by Hausleitner and Hafner [40], we model the interatomic couplings as in [32] by a volume dependent electron-gas term $E_{vol}(V)$ and pair potentials $\phi(r)$ adapted to the equilibrium distance, depth, width, and zero of the Hausleitner-Hafner potentials [40] for $Ni_{0.8}Zr_{0.2}$ [33]. For this model, simulations were started through heating a starting configuration up to 2000 K which leads to a homogeneous liquid state. The system then is cooled continuously to various annealing temperatures with cooling rate $-\partial_t T = 1.5 \ 10^{12}$ K/s. Afterwards the obtained configurations at various annealing temperatures (here 1500-600 K) are relaxed by carrying out additional isothermal annealing runs. Finally the time evolution of these relaxed configurations is modelled and analyzed. More details of the simulations are given in [33].

III. THEORY

A. Nonergodicity parameters

In this section we provide some basic formulae that permit calculation of T_c and the nonergodicity parameters $f_{ij}(q)$ for our system. A more detailed presentation may be found in Refs. [26, 27, 28, 41, 42]. The central object of the MCT are the partial intermediate scattering functions which are defined for a binary system by [43]

$$
\begin{aligned}
F_{ij}(q,t) &= \frac{1}{\sqrt{N_i N_j}} \left\langle \rho^i(q,t)\rho^j(-q,0) \right\rangle \\
&= \frac{1}{\sqrt{N_i N_j}} \sum_{\alpha=1}^{N_i} \sum_{\beta=i}^{N_j} \\
&\quad \times \left\langle \exp(i\mathbf{q} \cdot [\mathbf{r}_\alpha^i(t) - \mathbf{r}_\beta^j(0)]) \right\rangle \quad , \quad (1)
\end{aligned}
$$

where

$$
\rho_i(\overrightarrow{q}) = \sum_{\alpha=1}^{N_i} e^{i\overrightarrow{q} \cdot \overrightarrow{r}_{\alpha i}}, \ i = 1, 2 \quad (2)
$$

is a Fourier component of the microscopic density of species i.

The diagonal terms $\alpha = \beta$ are denoted as the incoherent intermediate scattering function

$$
F_i^s(q,t) = \frac{1}{N_i} \sum_{\alpha=1}^{N_i} \left\langle \exp(i\mathbf{q} \cdot [\mathbf{r}_\alpha^i(t) - \mathbf{r}_\alpha^i(0)]) \right\rangle \quad . \quad (3)
$$

The normalized partial- and incoherent intermediate scattering functions are given by

$$
\begin{aligned}
\Phi_{ij}(q,t) &= F_{ij}(q,t)/S_{ij}(q) \quad , & (4) \\
\Phi_i^s(q,t) &= F_i^s(q,t) \quad , & (5)
\end{aligned}
$$

where the $S_{ij}(q) = F_{ij}(q, t = 0)$ are the partial static structure factors.

The basic equations of the MCT are the set of nonlinear matrix integrodifferential equations

$$
\ddot{\mathbf{F}}(q,t) + \mathbf{\Omega}^2(q)\mathbf{F}(q,t) + \int_0^t d\tau \mathbf{M}(q, t-\tau)\dot{\mathbf{F}}(q,\tau) = 0 \quad , \quad (6)
$$

where $\mathbf{F}$ is the 2×2 matrix consisting of the partial intermediate scattering functions $F_{ij}(q,t)$, and the frequency matrix $\mathbf{\Omega}^2$ is given by

$$
\left[\mathbf{\Omega}^2(q)\right]_{ij} = q^2 k_B T(x_i/m_i) \sum_k \delta_{ik} \left[\mathbf{S}^{-1}(q)\right]_{kj} \quad . \quad (7)
$$

$\mathbf{S}(q)$ denotes the 2×2 matrix of the partial structure factors $S_{ij}(q)$, $x_i = N_i/N$ and m_i means the atomic mass of the species i. The MCT for the idealized glass transition

predicts [18] that the memory kern $\mathbf{M}$ can be expressed at long times by

$$M_{ij}(\mathbf{q},t) = \frac{k_B T}{2\rho m_i x_j} \int \frac{d\mathbf{k}}{(2\pi)^3} \sum_{kl}\sum_{k'l'}$$
$$\times V_{ikl}(\mathbf{q},\mathbf{k})V_{jk'l'}(\mathbf{q},\mathbf{q}-\mathbf{k})$$
$$\times F_{kk'}(\mathbf{k},t)F_{ll'}(\mathbf{q}-\mathbf{k},t) \quad , \qquad (8)$$

where $\rho = N/V$ is the particle density and the vertex $V_{i\alpha\beta}(\mathbf{q},\mathbf{k})$ is given by

$$V_{ikl}(\mathbf{q},\mathbf{k}) = \frac{\mathbf{q}\cdot\mathbf{k}}{q}\delta_{il}c_{ik}(\mathbf{k}) + \frac{\mathbf{q}\cdot(\mathbf{q}-\mathbf{k})}{q}\delta_{ik}c_{il}(\mathbf{q}-\mathbf{k}) \quad (9)$$

and the matrix of the direct correlation function is defined by

$$c_{ij}(\mathbf{q}) = \frac{\delta_{ij}}{x_i} - \left[\mathbf{S}^{-1}(\mathbf{q})\right]_{ij} \quad . \qquad (10)$$

The equation of motion for $F_i^s(q,t)$ has a similar form as Eq.(6), but the memory function for the incoherent intermediate scattering function is given by

$$M_i^s(\mathbf{q},t) = \int \frac{d\mathbf{k}}{(2\pi)^3}\frac{1}{\rho}\left(\frac{\mathbf{q}\cdot\mathbf{k}}{q}\right)(cF)_i(\mathbf{k},t)$$
$$\times F_i^s(\mathbf{q}-\mathbf{k},t), \qquad (11)$$

$$(cF)_i(k,t) = (c_{ii}(q))^2 F_{ii}(q,t) + 2c_{ii}(q)c_{ij}(q)F_{ij}(q,t)$$
$$+ (c_{ij}(q))^2 F_{jj}(q,t) \quad j \neq i \quad . \qquad (12)$$

In order to characterize the long time behaviour of the intermediate scattering function, the nonergodicity parameters $\mathbf{f}(\mathbf{q})$ are introduced as

$$f_{ij}(\mathbf{q}) = lim_{t\to\infty}\Phi_{ij}(\mathbf{q},t) \quad . \qquad (13)$$

These parameters are the solution of eqs. (6)-(10) at long times. The meaning of these parameters is the following: if $f_{ij}(\mathbf{q}) = 0$, then the system is in a liquid state with density fluctuation correlations decaying at long times. If $f_{ij}(\mathbf{q}) > 0$, the system is in an arrested, nonergodic state, where density fluctuation correlations are stable for all times. In order to compute $f_{ij}(\mathbf{q})$, one can use the following iterative procedure [28]:

$$\mathbf{f}^{(l+1)}(q) = \frac{\mathbf{S}(q)\cdot\mathbf{N}[\mathbf{f}^{(l)},\mathbf{f}^{(l)}](q)\cdot\mathbf{S}(q)}{\mathbf{Z}}$$
$$+ \frac{q^{-2}|\mathbf{S}(q)||\mathbf{N}[\mathbf{f}^{(l)},\mathbf{f}^{(l)}](q)|\mathbf{S}(q)}{\mathbf{Z}} \quad , \quad (14)$$

$$\mathbf{Z} = q^2 + Tr(\mathbf{S}(q)\cdot\mathbf{N}[\mathbf{f}^{(l)},\mathbf{f}^{(l)}](q))$$
$$+ q^{-2}|\mathbf{S}(q)||\mathbf{N}[\mathbf{f}^{(l)},\mathbf{f}^{(l)}](q)| \quad ,$$

where the matrix $\mathbf{N}(q)$ is given by

$$N_{ij}(q) = \frac{m_i}{x_i k_B T}M_{ij}(q) \quad . \qquad (15)$$

This iterative procedure, indeed, has two type of solutions, nontrivial ones with $\mathbf{f}(q) > 0$ and trivial solutions $\mathbf{f}(q) = 0$.

The incoherent nonergodicity parameter $f_i^s(q)$ can be evaluated by the following iterative procedure:

$$q^2 \frac{f_i^{s,l+1}(q)}{1 - f_i^{s,l+1}(q)} = M_i^s[\mathbf{f}, f_i^{s,l}](q) \quad . \qquad (16)$$

As indicated by Eq.(16), computation of the incoherent nonergodicity parameter $f_i^s(q)$ demands that the coherent nonergodicity parameters are determined in advance.

B. $\mathbf{g_m}$-parameter

Beyond the details of the MCT, equations of motion like (6) can be derived for the correlation functions under rather general assumptions within the Lanczos recursion scheme [44] resp. the Mori-Zwanzig formalism [45]. The approach demands that the time dependence of fluctuations A, B, ... is governed by a time evolution operator like the Liouvillian and that for two fluctuating quantitites a scalar products (B, A) with the meaning of a correlation function can be defined. In case of a tagged particle, this leads for $\Phi_i^s(q,t)$ to the exact equation

$$\ddot{\Phi}_i^s(q,t)/\Omega_0^2 + \Phi_i^s(q,t) + \int_0^t d\tau M_i^0(q,t-\tau)\dot{\Phi}_i^s(q,\tau) = 0 \qquad (17)$$

with memory kernel $M_i^0(q,t)$ in terms of a continued fraction.

Within $M_i^0(q,t)$ are hidden all the details of the time evolution of $\Phi_i^s(q,t)$. As proposed and applied in [24, 25], instead of calculating $M_i^0(q,t)$ from the time evolution operator as a continued fraction, it can be evaluated in closed forms once $\Phi_i^s(q,t)$ is known, e.g., from experiments or MD-simulations. This can be demonstrated by introduction of

$$\Phi_c(\omega) \pm i\Phi_s(\omega) := \lim_{\varepsilon\to 0}\mathcal{L}\{\Phi\}(\varepsilon \mp i\omega) \quad , \qquad (18)$$

with

$$\mathcal{L}\{\Phi\}(z) = \int_0^\infty dt e^{-zt}\Phi(t) \qquad (19)$$

the Laplace transform of $\Phi(t)$, and

$$M_i^0(\omega)_c \pm iM_i^0(\omega)_s := \lim_{\varepsilon\to 0}\mathcal{L}\{M_i^0\}(\varepsilon \mp i\omega) \quad . (20)$$

Eq.(17) then leads to

$$M_i^0(\omega)_c = \frac{\Phi_c(\omega)}{\left[1 - \omega\Phi_s(\omega)\right]^2 + \left[\omega\Phi_c(\omega)\right]^2} \quad . \qquad (21)$$

On the time axis, $M_i^0(t)$ is given by

$$M_i^0(t) = \frac{2}{\pi}\int_0^\infty d\omega M_i^0(\omega)_c \cos(\omega t) \quad . \qquad (22)$$

Adopting some arguments from the schematic MCT, Eq.(17) allows asymptotically finite correlations $\Phi_i^s(q,t \to \infty) > 0$, that means an arrested state, if $M_i^0(q,t \to \infty)$ remains finite where the relationship holds

$$M_i^0(q,t \to \infty)(\Phi_i^s(q,t \to \infty)^{-1} - 1) = 1 \quad . \quad (23)$$

In order to characterize the undercooled melt and its transition into the glassy state, we introduced in [24] the function

$$\mathbf{G}(\Phi, M^0) := M^0(t)(1/\Phi(t) - 1) \quad . \quad (24)$$

According to (23), $\mathbf{G}(\Phi, M^0)$ has the property that

$$\mathbf{G}(\Phi, M^0) \mid_{t \to \infty} = 1 \quad (25)$$

in the arrested, nonergodic state. On the other hand, if

$$\mathbf{g}_m := Max\left\{\mathbf{G}(\Phi, M^0) \mid 0 < t < \infty\right\} < 1 \quad , \quad (26)$$

there is no arrested solution and the correlations $\Phi_i^s(q,t)$ decay to zero for $t \to \infty$, that means, the system is in the liquid state. From that we proposed [24] to use the value of $\mathbf{g}_m$ as a relative measure how much the system has approached the arrested state and to use the temperature dependence of $\mathbf{g}_m(T)$ in the liquid state as an indication how the system approaches this state.

IV. RESULTS AND DISCUSSIONS

A. Partial structure factors and intermediate scattering functions

First we show the results of our simulations concerning the static properties of the system in terms of the partial structure factors $S_{ij}(q)$ and partial correlation functions $g_{ij}(r)$.

To compute the partial structure factors $S_{ij}(q)$ for a binary system we use the following definition [46]

$$S_{ij}(\overrightarrow{q}) = x_i\delta_{ij} + \rho x_i x_j \int (g_{ij}(r) - 1)e^{-i\overrightarrow{q}\cdot\overrightarrow{r}}d\overrightarrow{r} \quad (27)$$

where

$$g_{ij}(\overrightarrow{r}) = \frac{V}{N_i N_j}\left\langle \sum_{\alpha=1}^{N_i}\sum_{\beta=1,\beta\neq\alpha}^{N_j} \delta(\mathbf{r} - |\mathbf{r}_\alpha(t) - \mathbf{r}_\beta(t)|) \right\rangle \quad (28)$$

are the partial pair correlation functions.

The MD simulations yield a periodic repetition of the atomic distributions with periodicity length L. Truncation of the Fourier integral in Eq.(27) leads to an oscillatory behavior of the partial structure factors at small q. In order to reduce the effects of this truncation, we compute from Eq.(28) the partial pair correlation functions

for distance r up to $R_c = 3/2L$. For numerical evaluation of Eq.(27), a Gaussian type damping term is included

$$S_{ij}(q) = x_i\delta_{ij} + 4\pi\rho x_i x_j \int_0^{R_c} r^2(g_{ij}(r) - 1)\frac{\sin(qr)}{qr}$$
$$\times \exp(-(r/R)^2)dr \quad (29)$$

with $R = R_c/3$.

Fig.1- fig.3 shows the partial structure factors $S_{ij}(q)$ versus q for all temperatures investigated. The figure indicates that the shape of $S_{ij}(q)$ depends weakly on temperature only and that, in particular, the positions of the first maximum and the first minimum in $S_{ij}(q)$ are more or less temperature independent.
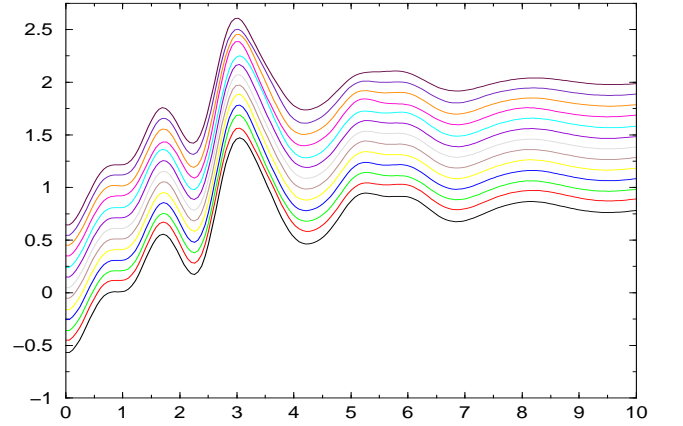

FIG. 1: Partial structure factors Ni-Ni-part at $T = 1500$ K, 1400 K, 1300 K, 1200 K, 1100 K, 1000 K, 900 K and 800 K (from top to bottom),the curves are vertically shifted by 0.05 relative to each other.
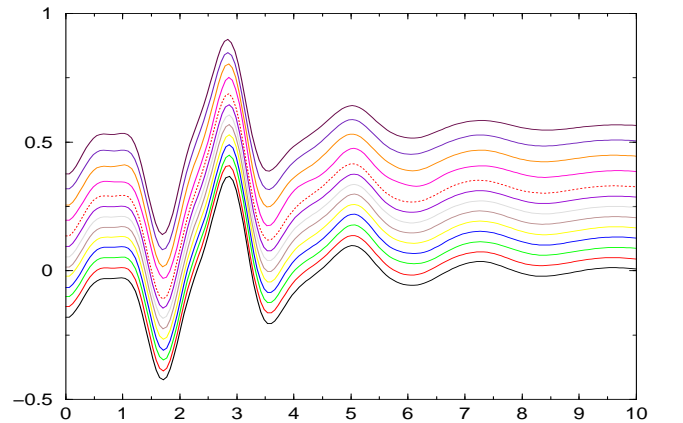

FIG. 2: Partial structure factors Ni-Zr-part at $T = 1500$ K, $T = 1400$ K, 1300 K, 1200 K, 1100 K, 1000 K, 900 K and 800 K (from top to bottom),the curves are vertically shifted by 0.05 relative to each other.

To investigate the dynamical properties of the system, we have calculated the incoherent scattering function
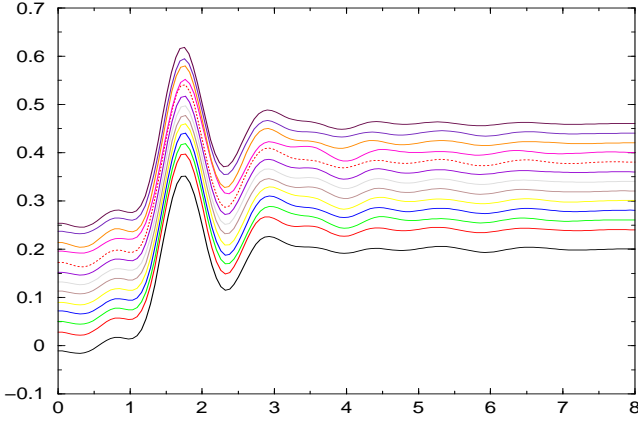
FIG. 3: Partial structure factors Zr-Zr-part at $T = 1500$ K, $T = 1400$ K, 1300 K, 1200 K, 1100 K, 1000 K, 900 K and 800 K (from top to bottom), the curves are vertically shifted by 0.05 relative to each other.

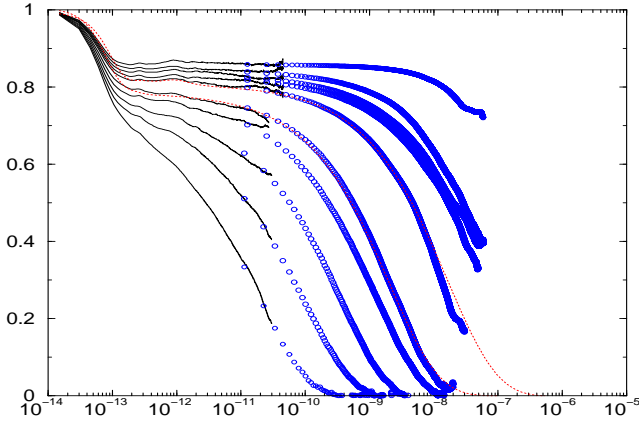$F_i^s(q,t)$ and the coherent scattering function $F_{ij}(q,t)$ as defined in equations (1) and (3).

FIG. 4: Incoherent intermediate scattering function $\Phi_i^s(q,t)$ Ni-part for $q = 24.4$ nm^{-1} at $T = 1500$ K, 1400 K, 1300 K, 1200 K, 1100 K, 1000 K, 950 K, 900 K, and 800 K (from left to right).

Fig.4 and fig.5 presents the normalized incoherent intermediate scattering functions $\Phi_i^s(q,t)$ of both species evaluated from our MD data for wave vector $q_n=2\pi n/L$ with n = 9, that means $q_9 = 24.4$ nm^{-1}. From the figure we see that $\Phi_i^s(q,t)$ of both species shows at intermediate temperatures a structural relaxation in three succesive steps as predicted by the idealized schematic MCT [47]. The first step is a fast initial decay on the time scale of the vibrations of atoms ($t < 0.2$ ps). This step is characterized by the MCT only globaly. The second step is the β-relaxation regime. In the early β-regime the correlator should decrease according to $\Phi_i^s(q,t) = f_{csi}(q)+A/t^a$ and in the late β-relaxation regime, which appears only in the melt, according the von Schweidler law $f_{csi}(q) - Bt^b$. Between them a wide plateau is found near the critical temperature T_c. In the melt, the α-relaxation takes
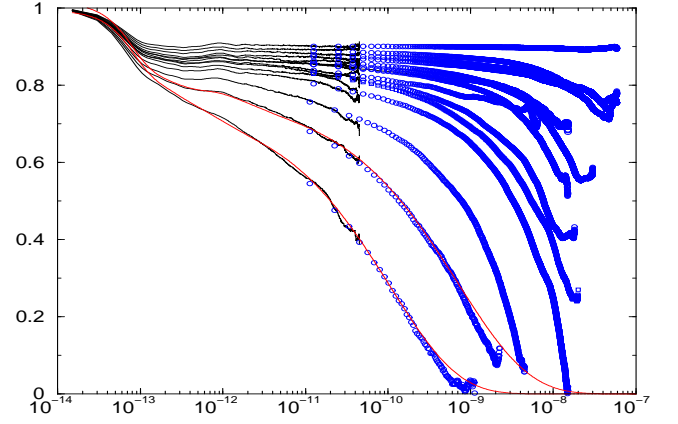
place as the last decay step after the von Schweidler-law. It can be described by the Kohlrausch-Williams-Watts (KWW) law $\Phi_i^s(q,t) = A_0 \exp(-(t/\tau_\alpha)^\beta)$ where the relaxation time τ_α near the glass transition shifts drastically to longer times.

The inverse power-law decay for the early β-regime $\Phi \sim f_c + A/t^a$ is not seen in our data. This seems to be due to the fact that in our system the power-law decay is dressed by the atomic vibrations ([24, 25] and references therein).

According to our MD-results, $\Phi_i^s(q,t)$ decays to zero for longer times at all temperatures investigated. This is in agreement with the full MCT. Including transversal currents as additional hydrodynamic variables, the full MCT [18] comes to the conclusion that all structural correlations decay in the final α-process, independent of temperature. Similar effects are expected from inclusion of thermally activated matter transport, that means diffusion in the arrested state.

At $T = 900$ K - 700 K, the $\Phi_i^s(q,t)$ drop rather sharply at large t. This reflects aging effects which take place, if a system is in a transient, non-steady state [48]. Such a behaviour indicates relaxations of the system on the time scale of the 'measuring time' of the correlations.

B. Nonergodicity parameters

The nonergodicity parameters are defined by Eq.(13) as a non-vanishing asymptotic solution of the MCT Eq.(6). Fig. 6 presents the estimated q-dependent nonergodicity parameters from the coherent and incoherent scattering functions of Ni and Zr at T=1005 K.

In order to compute the nonergodicity parameters $f_{ij}(q)$ analytically, we followed for our binary system the self-consistent method as formulated by Nauroth and Kob [28] and as sketched in Section III.A. Input data for our iterative determination of $f_{ij}(q) = F_{ij}(q,\infty)$ are the temperature dependent partial structure factors $S_{ij}(q)$ from the previous subsection. The iteration is started
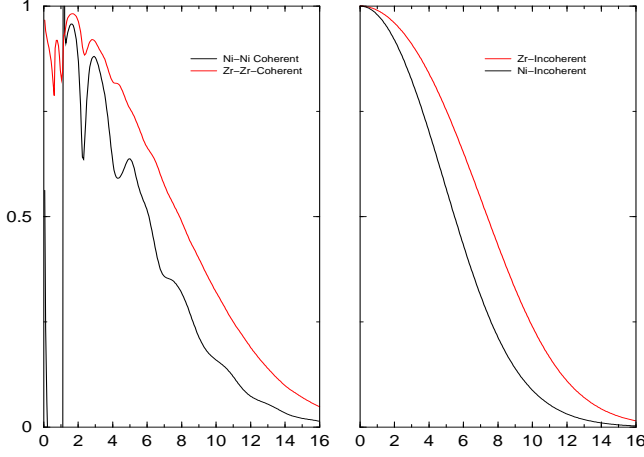

FIG. 5: The same as fig.4 but for Zr-part.

FIG. 6: Non-ergodicity parameter f_{cij} for the incoheremt and coherent intermediate scattering functions as solutions of eqs. (7) and (8)

by arbitrarily setting $F_{Ni-Ni}(q,\infty)^{(0)} = 0.5 S_{Ni-Ni}(q)$, $F_{Zr-Zr}(q,\infty)^{(0)} = 0.5 S_{Zr-Zr}(q)$, $F_{Ni-Zr}(q,\infty)^{(0)} = 0$.

For $T > 1100$ K we always obtain the trivial solution $f_{ij}(q) = 0$ while at T = 1000 K and below we get stable non-vanishing $f_{ij}(q) > 0$. The stability of the non-vanishing solutions was tested for more than 3000 iteration steps. From this results we expect that T_c for our system lies between 1000 and 1100 K. To estimate T_c more precisely, we interpolated $S_{ij}(q)$ from our MD data for temperatures between 1000 and 1100 K by use of the algorithm of Press et.al. [49]. We observe that at $T = 1005$ K a non-trivial solution of $f_{ij}(q)$ can be found, but not at $T = 1010$ K and above. It means that the critical temperature T_c for our system is around 1005 K. The non-trivial solutions $f_{ij}(q)$ for this temperature shall be denoted the critical nonergodicty parameters $f_{cij}(q)$. They are included in Fig. 6.

By use of the critical nonergodicity parameters $f_{cij}(q)$, the computational procedure was run to determine the critical nonergodicity parameters $f_{ci}^s(q)$ for the incoherent scattering functions at T = 1005 K . Fig. 6 also presents our results for the so calculated $f_{ci}^s(q)$.

C. $g(\Phi_i^s, M_i^0)$-function and g_m-parameters

Here we present our results about the $g(\Phi_i^s, M_i^0)$-function [24, 25] described in section III.B. The memory functions $M_i^0(q,t)$ are evaluated from the MD data for $\Phi_i^s(q,t)$ by Fourier transformation along the positive time axis. For completeness, also $T = 700$ and 800 K data are included where the corresponding $\Phi_i^s(q,t)$ are extrapolated to longer times by use of an KWW approximation.

Fig. 7 and Fig. 8 show the thus deduced $M_i^0(q,t)$ for $q = 24.4$ nm^{-1}. Regarding their qualitative features, the obtained $M_i^0(q,t)$ are in full agreement with the results
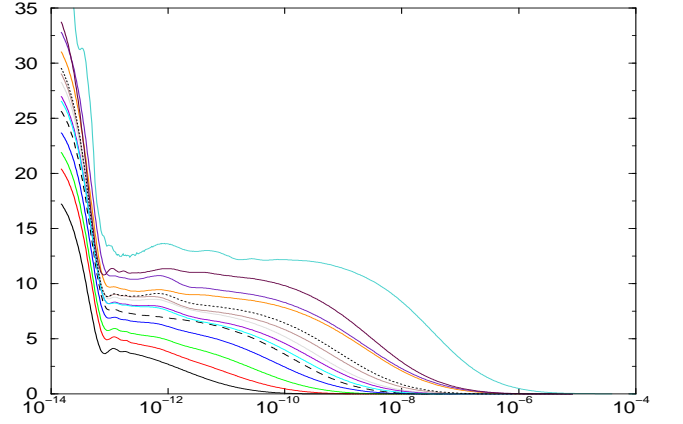

FIG. 7: Ni-Part: Time dependence of the dimensionless memory function $M_s^0(q,t)/\Omega_{s-i}^2$ from MD simulations for $q_9 = 21.6$ nm^{-1} and $T = 800$ K, 900 K, 950 K, 1000 K, 1100 K, 1200 K, 1300 K, 1400 K, and 1500 K (from top to bottom)
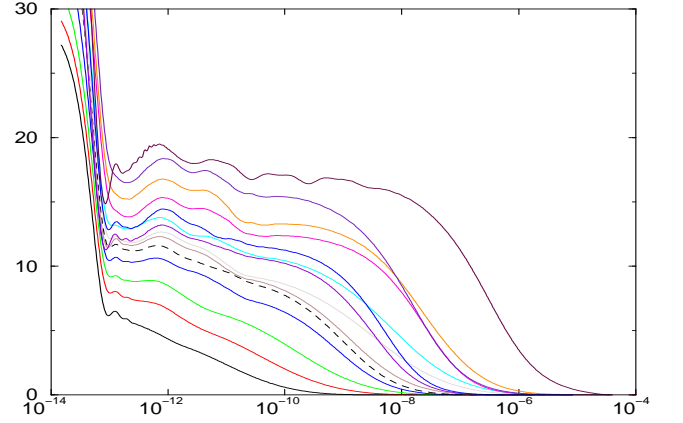

FIG. 8: The same as fig.7 but for Zr-part.

in [25] for the $Ni_{0.5}Zr_{0.5}$ system. A particular interesting detail is the fact that there exists a minimum in $M_i^0(q,t)$ for both species, Ni and Zr, at all investigated temperatures around a time of 0.1 ps. Below this time, $\Phi_i^s(q,t)$ reflects the vibrational dynamics of the atoms. Above this value, the escape from the local cages takes place in the melt and the β-regime dynamics are developed. Apparently, the minimum is related to this crossover.

In Fig. 9 and Fig. 10 we display $M_i^0(q, \Phi_i^s(q,t))$, that means $M_i^0(q,t)$ versus $\Phi_i^s(q,t)$. In this figure we again find the features already described for $Ni_{0.5}Zr_{0.5}$ in [24, 25]. According to the plot, there exist (q-dependent) limiting values $\Phi_{i0}^s(q,t)$ so that $M_i^0(q,t)$ for $\Phi_i^s(q,t) < \Phi_{i0}^s(q,t)$ is close to an universal behavior, while for $\Phi_i^s(q,t) > \Phi_{i0}^s(q,t)$ marked deviations are seen. $\Phi_{i0}^s(q,t)$ significantly decreases with increasing temperature. It is tempting to identify $M_i^0(q,t)$ below $\Phi_{i0}^s(q,t)$ with the polynomial form for $M_i^0(q,t)$ assumed in the schematic version of the MCT [18]. In fig. 9 and fig. 10, the polynomial obtained by fitting the 1000 K data be-
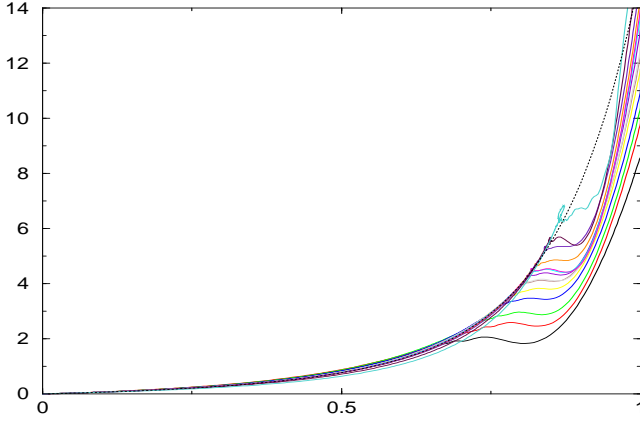
FIG. 9: Ni-Part: Dimensionless memory function $M_s^0(q,t)/\Omega_{s-i}^2$ as a function of $\Phi_i^s(q,t)$ (solid line) for $q_9 = 24.4$ nm^{-1} and $T = 800$ K, 900 K, 950 K, 1000 K, 1100 K, 1200 K, 1300 K, 1400 K, and 1500 K (from top to bottom); a) Ni-part and b) Zr-part ; Polynom fit of the low Φ memory function $M(\Phi)$ at $T = 800$ K (long dashed line).

FIG. 10: The same as fig.9 but for Zr-part.

at the present high temperatures.

FIG. 11: Ni-part: MD simulation results for the characteristic function $\mathbf{g}(\Phi^s)$ as a function of Φ_i^s for $q = 24.4$ nm^{-1}
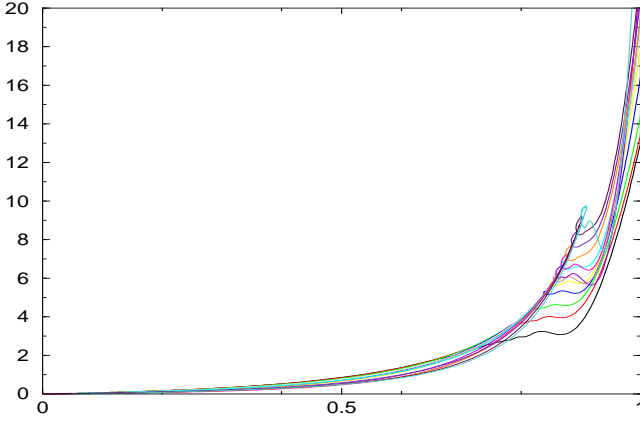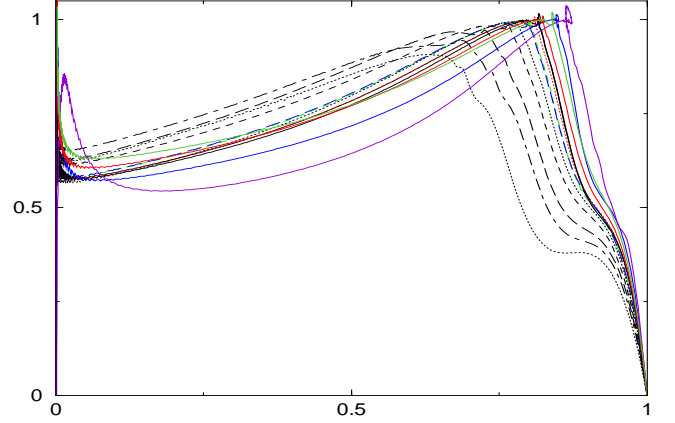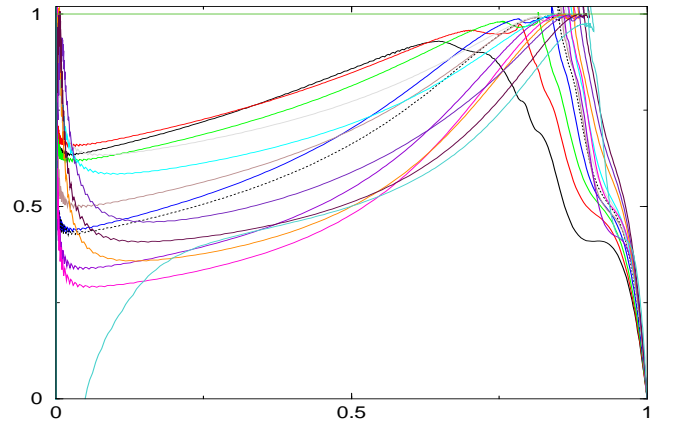

FIG. 12: The same as fig.11 but for Zr-part.

low $\Phi_{i0}^s(q,t)$ is included by a dashed line, extrapolating it over the whole Φ-range.

By use of the calculated memory functions, we can evaluate the $\mathbf{g}(\Phi_i^s, M_i^0)$, Eq.(24). In Fig.11 and Fig. 12 this quantity is presented versus the corresponding value of $\Phi_i^s(q,t)$ and denoted as $\mathbf{g}(\Phi_i^s)$. For all the investigated temperatures, $\mathbf{g}(\Phi_i^s)$ has a maximum $\mathbf{g}_m(q,T)$ at an intermediate value of Φ. In the high temperature regime, the values of $\mathbf{g}_m(q,T)$ move with decreasing temperature towards the limiting value 1. This is, in particular, visible in Fig. 13 where we present $\mathbf{g}_m(q,T)$ as function of temperature for both species, Ni and Zr, and wave-vectors $q_9 = 24.4$ nm^{-1}. At temperatures above 1000 K, the $\mathbf{g}_m$-values increase approximately linear towards 1 with decreasing temperatures. Below 1000 K, they remain close below the limiting value of 1, a behavior denoted in [24, 25] as a balancing on the borderline between the arrested and the non-arrested state due to thermally induced matter transport by diffusion in the arrested state

Linear fit of the $\mathbf{g}_m$-values for Ni above 950 K and for Zr above 1000 K predicts a crossover temperature T_c^* from liquid ($\mathbf{g}_m < 1$) to the quasi-arrested ($\mathbf{g}_m = 1$) behavior around 970 K from the Ni data and around 1020 K from the Zr data. We here identify this crossover temperature with the value of T_c as visible in the ergodic, liquid regime and estimate it by the mean value from the Ni- and Zr-subsystems, that means by $T_c = 1000$ K.

While in [24, 25] for the Ni$_{0.5}$Zr$_{0.5}$ melt a T_c-value of 1120 K was estimated from $\mathbf{g}_m(T)$, the value for the present composition is lower by about 120 K. A significant composition dependence of T_c is expected according to the results of MD simulation for the closely related Co$_x$Zr$_{1-x}$ system [15]. Over the whole x-range, T_c was found to vary between 1170 and 650 K in Co$_x$Zr$_{1-x}$, with $T_c(x = 0.2) \simeq 800$ K. Regarding this, the present data for the Ni$_x$Zr$_{1-x}$ system reflect a rather weak T_c variation.
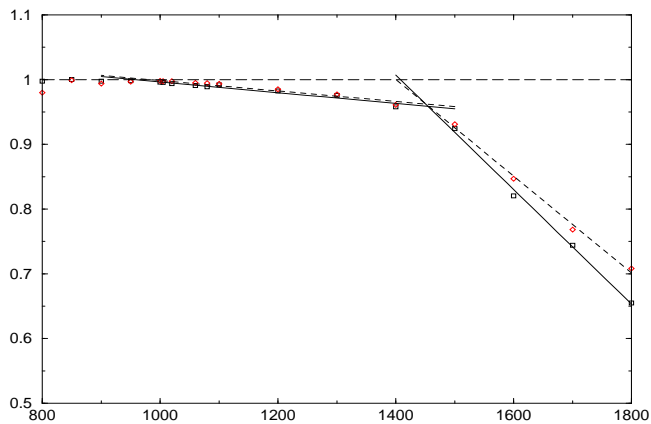
FIG. 13: MD simulation results of the temperature dependence of $\mathbf{g}_m(q,T)$ for $q_9 = 24.4$ nm^{-1} (symbols). Linear fits to the $\mathbf{g}_m(q,T)$ are included by full and dash lines (for $q_9 = 24.4$ nm^{-1}); a) Zr-part with $T_c = 970$ K and b) Ni-part with $T_c = 950$ K.

D. Diffusion-coefficients

From the simulated atomic motions in the computer experiments, the diffusion coefficients of the Ni and Zr species can be determined as the slope of the atomic mean square displacements in the asymptotic long-time limit

$$D_i(T) = \lim_{t \to \infty} \frac{(1/N_i) \sum_{\alpha=1}^{N_i} |\mathbf{r}_\alpha(t) - \mathbf{r}_\alpha(0)|^2}{6t} \quad . \quad (30)$$

Fig. 14 shows the thus calculated diffusion coefficients of our $Ni_{0.8}Zr_{0.2}$ model for the temperature range between 600 and 2000 K. At temperatures above approximately 1000 K, the diffusion coefficients for both species run parallel to each other in the Arrhenius plot, indicating a fixed ratio $D_{Ni}/D_{Zr} \approx 2.5$ in this temperature regime. At lower temperatures, the Ni atoms have a lower mobility than the Zr atoms, yielding around 800 K a value of about 10 for D_{Ni}/D_{Zr}. That means, here the Zr atoms carry out a rather rapid motion within a relative immobile Ni matrix.

According to the MCT, above T_c the diffusion coefficients follow a critical power law

$$D_i(T) \sim (T - T_c)^\gamma, \text{ for } T > T_c \quad (31)$$

with non-universal exponent γ [50].

In order to estimate T_c from this relationship, we have adapted the critical power law by a least mean squares fit to the simulated diffusion data for 1000 K and above. According to this fit, the system has a critical temperature of about 850-900 K.

Similar results for the temperature dependence of the diffusion coefficients have been found in MD simulations for other metallic glass forming systems, e.g., for $Ni_{0.5}Zr_{0.5}$ [33], for Ni_xZr_{1-x} [15], $Cu_{0.33}Zr_{0.67}$ [51], or $Ni_{0.81}B_{0.19}$ [52]. In all cases, like here, a break is observed
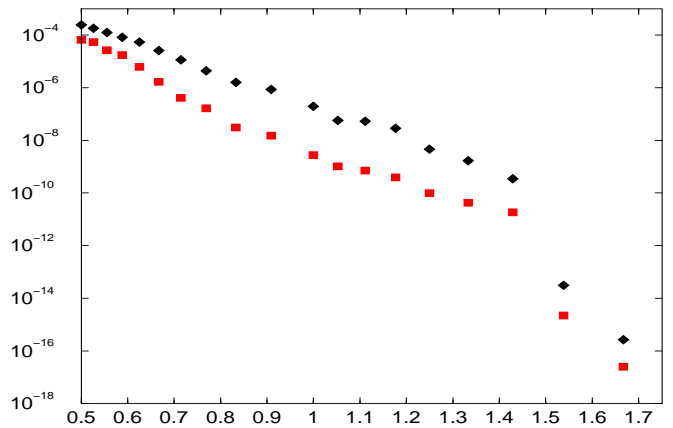

FIG. 14: Diffusion coefficients D_i as a function of $1000/T$. Symbols are MD results for Zr (squares) and Ni (diamonds)

in the Arrhenius slope. In the mentioned Zr-systems, this break is related to a change of the atomic dynamics around T_c whereas for $Ni_{0.81}B_{0.19}$ system it is ascribed to T_G. As in [52] T_c and T_G apparently fall together, there is no serious conflict between the obervations.

V. CONCLUSION

The present contribution reports results from MD simulations of a $Ni_{0.8}Zr_{0.2}$ computer model. The model is based on the electron theoretical description of the interatomic potentials for transition metal alloys by Hausleitner and Hafner [40]. There are no parameters in the model adapted to the experiments.

There is close agreement between the T_c values estimated from the dynamics in the undercooled melt when approaching T_c from the high temperature side. The values are $T_c \approx 950 - 1020$ K from the $\mathbf{g}_m$-parameters, and $T_c \approx 950$ K from the diffusion coefficients. As discussed in [15], the T_c-estimates from the diffusion coefficients seem to depend on the upper limit of the temperature region taken into account in the fit procedure, where an increase in the upper limit increases the estimated T_c. Accordingly, there is evidence that the present value of 950 K may underestimate the true T_c by about 10 to 50 K, as it based on an upper limit of 2000 K only. Taking this into account, the present estimates from the melt seem to lead to a T_c value around 1000 K.

The T_c from the nonergodicity parameters describe the approach of the system towards T_c from the low temperature side. They predict a T_c value of 1005 K. This value is clearly outside the range of our T_c estimates from the high temperature, ergodic melt. We consider this as a significant deviation which, however, is much smaller than the factor of two found in the modelling of a Lennard-Jones system [28]. The here observed deviation between the T_c estimates from the ergodic and the so-called nonergodic side reconfirm the finding from the soft spheres model[27] of an agreement within some 10 % between the

different T_c-estimates.

Acknowledgments

---

[1] W. Götze and M. Sperl, J. Phys.: Condens. Matter **16**, 4807 (2004); W. Götze and M. Sperl, Phys.Rev.Lett. **92**, 105701 (2004)

[2] P. G. Debenedetti and F.H. Stillinger, Nature **410**(6825), 259 (2001).

[3] M. Mezard and G. Parisi, Phys.Rev.Lett. **82**(4), 747 (1999).

[4] J.H. Gibbs and E. A. DiMarzio, J.Chem.Phys. **28**(3), 373 (1958).

[5] B.Colluzi, G.Parisi, and P.Verrochio, Phys.Rev.Lett. **84**(2), 306(2000).

[6] T. S. Grigera and G. Parisi, Phys. Rev. E **63**, 045102(R) (2001).

[7] L. Santen and W. Krauth, Nature **405**(6786), 550 (2000).

[8] W. Götze and L. Sjögren, Rep. Prog. Phys. **55**(3), 241 (1992)

[9] W. Kob und H.C. Andersen, Phys. Rev. E **51**(5), 4626 (1995).

[10] S. Sastry, P. G. Debendetti and F. H. Stillinger, Nature **393**(6685), 554 (1998).

[11] F. Sciortino, W. Kob, and P. Tartaglia, Phys. Rev. Lett. **83**(16), 3214 (1999).

[12] C. Donati, S. C. Glotzer, P. H. Poole, W. Kob, and S. J. Plimpton, Phys.Rev. E **60**(3), 3107 (1999)

[13] B. Colluzi, G. Parisi, and P. Verrochio, Phys. Rev. Lett. **112**(6), 2933 (2000).

[14] R. Yamamoto and W. Kob, Phys.Rev. E **61**(5), 5473 (2000)

[15] U. Rössler and H. Teichler, Phys. Rev. B **61**, 394 (2000).

[16] U. Bengtzelius, W. Götze, and A. Sjölander, J. Phys. C **17**, 5915 (1984).

[17] E. Leutheusser, Phys. Rev. A **29**, 2765 (1984).

[18] W. Götze and L. Sjögren, Rep. Prog. Phys. **55**, 241 (1992)

[19] P.S. Das and G.F. Mazenko, Phys. Rev. A **34**, 2265 (1986).

[20] L. Sjögren, Z. Phys. B **79**, 5 (1990).

[21] T. Gleim and W. Kob, Eur. Phys. J. B **13**, 83 (2000).

[22] A. Meyer, R. Busch, and H. Schober, Phys. Rev. Lett. **83**, 5027 (1999); A. Meyer, J. Wuttke, W. Petry, O.G. Randl, and H. Schober, Phys. Rev. Lett. **80**, 4454 (1998).

[23] H.Z. Cummins, J. Phys.Cond.Mat. **11**, A95 (1999).

[24] H. Teichler, Phys. Rev. Lett. **76**, 62(1996).

[25] H. Teichler, Phys. Rev. E **53**, 4287 (1996).

[26] J.L. Barrat and A. Latz, J. Phys. Cond. Matt. **2**, 4289 (1990).

[27] M. Fuchs, Thesis, TU-Muenchen (1993); M. Fuchs and A. Latz, Physica A **201**, 1 (1993).

[28] M. Nauroth and W. Kob, Phys. Rev. E **55**, 657 (1997).

[29] M. Kuschke, Thesis, Universität Stuttgart (1991).

[30] Yan Yu, W.B. Muir and Z. Altounian, Phys. Rev. B **50**, 9098 (1994).

[31] B. Böddeker, Thesis, Universität Göttingen (1999); Böddeker and H. Teichler, Phys. Rev. E **59**, 1948 (1999)

[32] H. Teichler, phys. stat. sol. (b) **172**, 325 (1992)

[33] H. Teichler, in: *Defect and Diffusion Forum* **143-147**, 717 (1997)

[34] H. Teichler, in: *Simulationstechniken in der Materialwissenschaft*, edited by P. Klimanek and M. Seefeldt (TU Bergakadamie, Freiberg, 1999).

[35] H. Teichler, Phys. Rev. B **59**, 8473 (1999).

[36] T. Aihara, K. Aoki and T. Masumoto, Material Trans., JIM **36**, 399 (1995)

[37] T. Aihara, Y. Kawazoe and T. Masumoto, Sci. Rep. RITU A **41**, 1 (1995)

[38] T. Aihara and T. Masumoto, J. Phys. Cond. Mat. **7**, 1525 (1995)

[39] T. Aihara, Y. Kawazoe and T. Masumoto, Sci. Rep. RITU A **42**, 57 (1996)

[40] Ch. Hausleitner and Hafner, Phys. Rev. B **45**, 128 (1992).

[41] W. Götze, Z. Phys. B **60**, 195 (1985).

[42] J. Bosse and J.S. Thakur, Phys. Rev. Lett. **59**, 998 (1987).

[43] B. Bernu, J.-P. Hansen, G. Pastore, and Y. Hiwatari, Phys. Rev A **36**, 4891 (1987); ibid. **38**, 454 (1988).

[44] C. Lanczos. J. Res. Natl. Bur. Stand. **45**, 255 (1950).

[45] R. Zwanzig, J. Chem. Phys. **33**, 1338 (1960); H. Mori, Prog. Theor. Phys. **33**, 423 (1965)

[46] J.P. Hansen and I.R. McDonald, *Theory of Simple Liquids*, 2nd Ed. (Academic Press, London, 1986).

[47] J.-P. Hansen and S. Yip, Transp. Theory Stat. Phys. **24**, 1149 (1995).

[48] W. Kob and J.L. Barrat, Physica A **263**, 1 (1999); Phys. Rev. Lett. **78**, 4581 (1997).

[49] W.H. Press, B.P. Flannery, S.A. Teukolsky and W.T. Vetterling, *Numerical Recipes*, 2nd.Edition (University Press, Cambrigde, New York, 1992).

[50] W. Kob and H.C. Andersen, Phys. Rev. E **51**, 4626 (1995).

[51] C. Gaukel, Thesis, TU-Aachen (1998).

[52] L.D. van Ee, Thesis, TU-Delft (1998).